FOURIER FILTERING IN A BAROTROPIC POLAR OCEAN MODEL

Satoshi SAKAI* and Shiro IMAWAKI

Geophysical Institute, Kyoto University, Sakyo-ku, Kyoto 606

Abstract: A Fourier filtering is examined in a polar ocean model based on the vorticity equation. A circular basin centered at the North Pole is considered. Flows are driven by an inflow and an outflow prescribed at the circumference. Two peninsulas are provided for examination of the filtering effect. In a slip boundary case, longitudinal distribution of the predicted vorticity is expanded in sine series and high wavenumber components are eliminated. The solution obtained with the filtering agrees well with that obtained without filterings. In a viscous boundary case, the vorticity is expanded in cosine series and high wavenumber components are eliminated. The filtering does not affect the general flow pattern, although it slightly affects the local vorticity field near irregular coastal boundaries.

1. Introduction

Since the heat budget in the Arctic Ocean has a significant effect on the global climate changes, a number of numerical models of the Arctic Ocean have been presented (CAMPBELL, 1965; GALT, 1973; SEMTNER, 1976). Numerical sea-ice models have been presented by ROTHROCK (1975), PARKINSON and WASHINGTON (1979), and HIBLER (1979). In these models, local Cartesian coordinates or some particular coordinates were adopted. For a polar ocean model, however, spherical coordinates are most desirable because the dynamics of the Arctic Ocean and the Antarctic Ocean should be finally studied in relation to the global ocean-atmosphere circulation.

In a model described in spherical coordinates, the grid points are closely spaced near the Pole and a very short time step is required for the computational stability in the time integration. So far a few methods have been presented to relax the restriction. ARAKAWA (1972) applied a filter to the zonal mass flux variables and the zonal pressure gradient term for eliminating high frequency gravity waves in a global atmospheric circulation model. HOLLOWAY *et al.* (1973) successfully used a Fourier filtering to ensure the stability and were able to take a large time step in their global atmosphere model. The basic idea of filtering is to make the spatial resolution uniform all over the computational domain by eliminating high wavenumber components.

* Present affiliation: Institute of Earth Science, Kyoto University, Sakyo-ku, Kyoto 606.

An ocean model differs from an atmosphere model in the existence of lateral boundaries. In some cases, boundary conditions remarkably affect flows in the basin (for example, BLANDFORD, 1971). BRYAN *et al.* (1975) used the filtering in a three-dimensional ocean model; they expanded the velocity components in sine series in the longitudinal direction with the both ends at a coastal boundary, so as to satisfy a viscous boundary condition.

In the present paper we study the filtering in a two-dimensional polar ocean model based on the vorticity equation on spherical coordinates. A polar ocean of simplified geometry is considered for clearly examining the effects of the filtering. Solutions obtained with the filtering are compared with those obtained without filterings in the cases of a slip boundary and a viscous boundary.

2. Description of the Model

A circular basin centered at the North Pole is considered. Figure 1 shows the basin schematically. The circumference is a 70°N latitude circle. There are two openings on the circumference. The flow in the basin is driven by an inflow and an outflow through these openings. Their volume transports ψ_0 are constant in time. There are two peninsulas extending near to the Pole, which introduce western boundary currents.

The flow is assumed to be horizontally nondivergent. The vorticity equation is

$$\frac{\partial \zeta}{\partial t} = \boldsymbol{J}(\zeta + f, \psi) + A\nabla^2\zeta \tag{1}$$

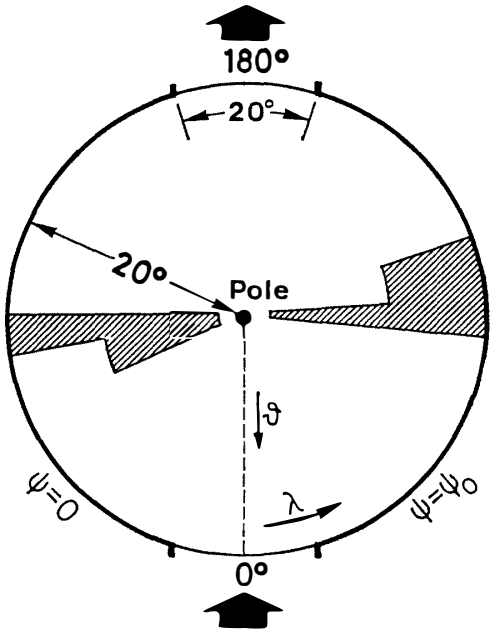

Fig. 1. Schematic figure of a polar ocean provided for examination of the Fourier filtering. Flows are driven by an inflow and an outflow prescribed at two openings. Two peninsulas extend near to the Pole.

where ζ is the relative vorticity, f the Coriolis parameter, A the eddy viscosity coefficient, ψ the stream function, $\boldsymbol{J}(\zeta, \psi)$ the Jacobian operator, and ∇^2 the Laplacian in the spherical form. The finite difference form of the time derivative in eq. (1) is written as

$$\frac{\zeta_{j+1}-\zeta_{j-1}}{2\Delta t}=\boldsymbol{J}_j(\zeta+f, \psi)+A\nabla^2\zeta_{j-1} \tag{2}$$

where j denotes time step. The finite difference form of $\boldsymbol{J}$ is defined according to ARAKAWA (1966) so that the total vorticity, the total square vorticity and the total kinetic energy are conserved. The longitudinal grid size $\Delta\lambda$ is set as five degrees, which corresponds to about 190 km grid spacing at the circumference and about 19 km grid spacing at the grid points nearest to the Pole. The latitudinal grid size $\Delta\theta$ is set as two degrees, which corresponds to about 220 km spacing. The eddy viscosity coefficient A is set as 10^8 cm^2/s. The volume transport ψ_0 is set so as to make the velocities at the inlet and the outlet 13 cm/s.

The computational stability condition in the control runs in which no filtering is used is given as

$$\left(\omega+\frac{4A(1+\gamma^2)}{(R\Delta\lambda\sin\theta)^2}+\frac{U}{R\Delta\lambda\sin\theta}+\frac{V}{R\Delta\theta}\right)\cdot\Delta t<1 \tag{3}$$

where ω is the maximum frequency of the Rossby-Haurwitz wave, R the radius of the earth, γ the ratio of the longitudinal grid spacing to the latitudinal one ($\gamma=\Delta\lambda\sin\theta/\Delta\theta$), U the maximum longitudinal velocity component and V the maximum latitudinal one. The first term in the parentheses represents the stability condition on the Rossby-Haurwitz wave. The maximum frequency of this wave in the present basin without the peninsulas is 1.3×10^{-6}s^{-1} (SAKAI and IMAWAKI, 1980). The second term represents the stability condition for the viscous term. It has the maximum value at the grid points nearest to the Pole. The third term and the fourth term represent the restriction due to the vorticity advection term. When U and V are 10 cm/s, eq. (3) gives $\Delta t<0.103$ day. Hence the time step is set as 0.1 day in the control runs. This severe restriction is due to the viscous term; the second term is greater than other terms by one order of magnitude. A well-known explicit method for removing the restriction due to the viscous term is the method of DUFORT and FRANKEL (1953). This method is always stable for heat equation regardless of time step and has been used successfully in a great number of fluid-dynamics problems. The method, however, is easily made unstable by the advection term or some other terms when the grid spacing is too small as is in the present case. The restriction on time step in the present case is relaxed by the Fourier filtering as follows. The longitudinal distribution of predicted vorticity is expanded in Fourier series at each time step and its higher wavenumber components than cut-off wavenumber are eliminated. The cut-off wavenumber is determined so that the longitudinal resolution in length

is the same as the latitudinal one.

For a slip boundary, the vorticity is zero at the boundary because the viscous stress tangential to the boundary $\rho A\zeta$ (ρ is the density) is zero at the boundary. The vorticity is expanded in sine series and high wavenumber components are excluded. The filtered vorticity also gives no tangential stress at the boundary; the slip boundary condition is satisfied after the filtering.

On the other hand, there are no restrictions on the vorticity for a viscous boundary condition, which require the velocity to be zero at the boundary. In this case, the vorticity is expanded in cosine series and high wavenumber components are excluded. The filtered vorticity gives non-zero velocities at the boundary in general; the viscous boundary condition is not exactly satisfied after the filtering. The error, however, is small if the substantial resolution is so fine that the physical phenomenon of the smallest scale in the model can be resolved well.

The stability condition reduces to

$$\left(\omega+\frac{8A}{(\Delta x^*)^2}+\frac{U^*}{\Delta x^*}\right)\cdot\Delta t<1 \tag{4}$$

where Δx^* is the cut-off scale (the minimum scale of horizontal variation of ζ after the filtering) and U^* the maximum value of the horizontal velocity. This equation gives $\Delta t<3.1$ day. The time step is set as 2.5 day in the filtering run.

3. Results

Time integrations are carried out for 250 days in both the control runs and the filtering runs for the slip boundary condition and the viscous boundary condition. As the initial condition a potential flow is specified, whose vorticity is zero everywhere in the basin.

At the initial stage of the time integration, the Rossby-Haurwitz waves are generated and propagated to the west. The waves vanish after several times of reflection and flows approach the steady state. The phase speed of the Rossby-Haurwitz wave in the filtering runs slightly differs from that of the control runs because the larger time step results in a slightly higher phase speed of the wave. Therefore, it is inadequate to examine the errors due to the spatial filtering at the early stage. Discussions are confined to the solutions in almost steady states.

The flow patterns in almost steady states (at 250 days) for the viscous boundary condition are shown in Fig. 2. Western boundary currents are clearly seen on the eastern sides of the peninsulas. At first sight, the difference in the flow patterns between the filtering run and the control run is scarecely recognizable. The same is true in the solutions for the slip boundary condition (not shown).

Figure 3 shows zonal distributions of vorticity at $\theta=8°$ in the viscous boundary

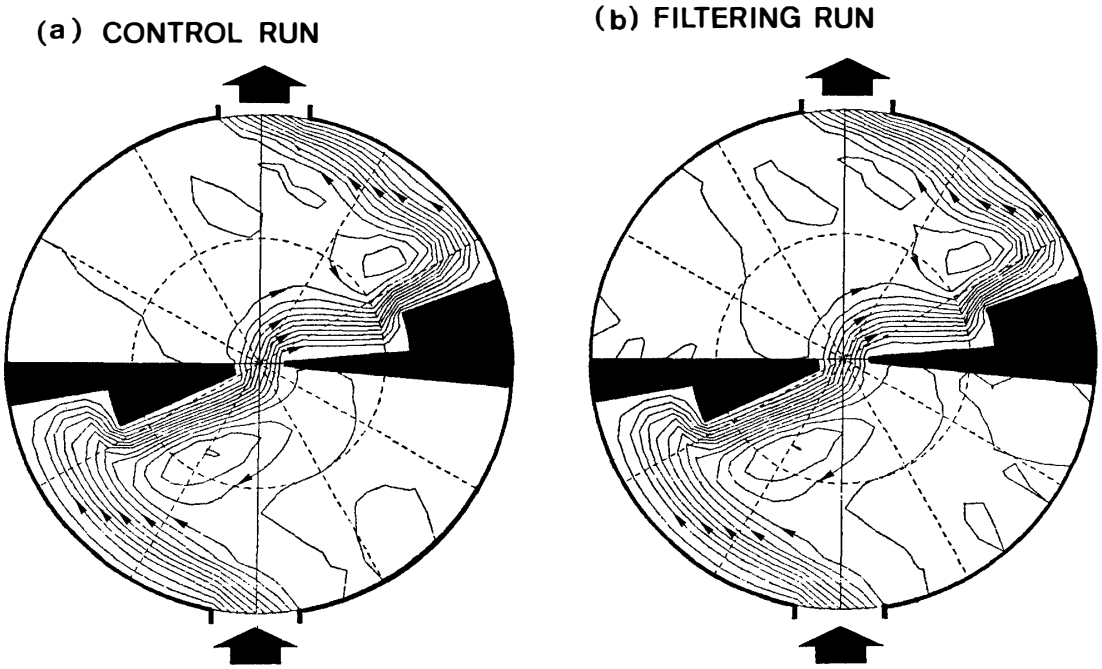

Fig. 2. Stream lines in the almost steady state (at 250 days) in the viscous boundary case, (a) obtained without filterings and (b) obtained with the Fourier filtering.

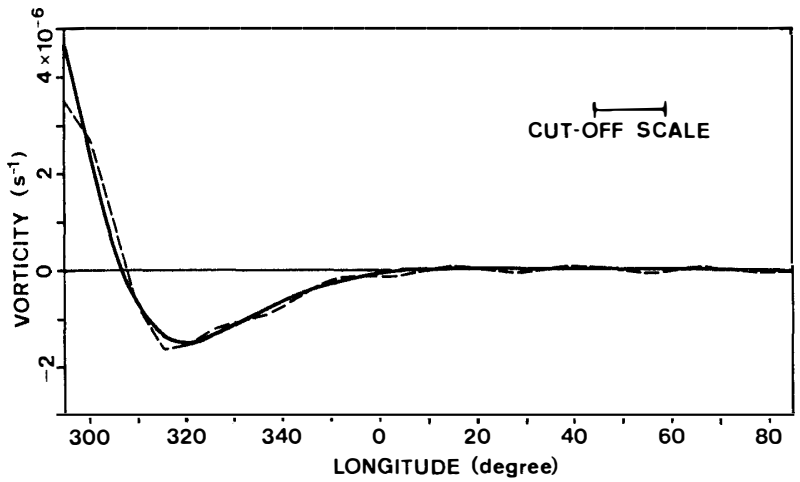

Fig. 3. Zonal distribution of vorticity at $\theta=8°$ in the viscous boundary case. A solid line is the distribution in the control run and a broken line is that in the filtering run. The cut-off scale is aslo shown.

case. The vorticity distribution in the filtering run (broken line) agrees well in general with that in the control run (solid line). In the filtering run, a smaller scale structure of vorticity than the cut-off scale can not be resolved, and wave-like errors are intro-

duced. The present focus of discussions is how the filtering affects the larger scale structure than the cut-off scale.

Two indices of filtering effect are now introduced as

$$\alpha_G = |\Delta\psi_{WB}|/\psi_0$$
$$\alpha_L = \max|\Delta\zeta|/\max|\zeta|$$

where $\Delta\psi_{WB}$ is the difference in the maximum volume transport of the western boundary currents between the control run and the corresponding filtering run, and $\Delta\zeta$ the difference in the vorticity field between the two runs. Here the vorticity in the control run is also filtered spatially because small scale variation which is excluded in the filtering run should be removed in the comparison. The index α_G is considered to represent the difference in the general flow pattern and the index α_L is considered to represent the difference in the local flow pattern. The indices for the slip and viscous boundary conditions are shown in Table 1.

Table 1. Indices of filtering effect.

	Slip boundary	Viscous boundary
α_G	Less than 2%	0.3%
α_L	1%	4%

In the slip boundary case, the Rossby-Haurwitz wave has not completely vanished. The relatively large value of 2% of α_G is mainly due to the phase speed difference of the Rossby-Haurwitz wave mentioned above and the magnitude of α_G concerning the spatial filtering is much smaller than it.

In the viscous boundary case, α_G is fairly small. Locations of the centers of gyres near the western boundaries in the filtering run are the same as those in the control run (see Fig. 2). The difference in the vorticity field between the two runs is largest near the capes of the peninsulas, because the capes are too sharp for the flows to be resolved well. Except for these areas, α_L has a value of 4% near the protrusions of the peninsulas at $\theta=12°$.

4. Conclusion

In the slip boundary case, no significant differences between the control run and the filtering run are recognized except the slight difference due to the modified phase speed of the Rossby-Haurwitz wave, which depends on the time resolution.

In the viscous boundary case, the filtering little affects the general flow pattern. The local vorticity field is slightly affected near the irregular coasts; the value of 4% of α_L may not be negligibly small. Widths of the western boundary currents are wider

in the viscous boundary case than in the slip boundary case, but a finer resolution seems to be required in the viscous boundary case. This is because the boundary is a line source of the vorticity and relatively high wavenumber components of the vorticity field are somewhat important. The value of α_L depends also on nonlinearity of the model, because in a linear case Fourier components are independent of each other and the filtering does not affect lower wavenumber components than the cut-off wavenumber.

In summary, Fourier filtering does not significantly distort the numerical solution in both the viscous and slip boundary cases in the present model, where the parameters representative of the polar ocean are used, although its effect might be significant in a highly nonlinear viscous case.

Acknowledgments

The authors wish to thank Prof. H. KUNISHI of Kyoto University for his guidance and encouragement. Prof. K. TAKANO of the University of Tsukuba is also acknowledged for his helpful advice. The authors are much indebted to reviewers for their critical reading of the manuscript. The numerical computations were carried out on a FACOM M-200 at the Data Processing Center, Kyoto University. This work was done under the Polar Experiment (POLEX) program.

References

ARAKAWA, A. (1966): Computational design for long-term numerical integration of the equation of fluid motion: Two-dimensional incompressible flow. Part I. J. Comput. Phys., **1**, 119–143.

ARAKAWA, A. (1972): Design of UCLA general circulation model. Technical Report No. 7, Numerical Simulation of Weather and Climate. Los Angeles, Dept. Meteorol., Univ. California, 116 p.

BLANDFORD, R. R. (1971): Boundary conditions in homogeneous ocean models. Deep-Sea Res., **18**, 739–751.

BRYAN, K., MANABE, S. and PACANOWSKI, R. C. (1975): A global ocean-atmosphere climate model. Part II. The oceanic circulation. J. Phys. Oceanogr., **5**, 30–46.

CAMPBELL, W. J. (1965): The wind-driven circulation of ice and water in a polar ocean. J. Geophys. Res., **70**, 3279–3301.

DUFORT, E. C. and FRANKEL, S. P. (1953): Stability conditions in the numerical treatment of parabolic differential equations. Math. Tables Other Aids Comput., **7**, 135–152.

GALT, J. A. (1973): A numerical investigation of Arctic Ocean dynamics. J. Phys. Oceanogr., **3**, 379–396.

HIBLER, W. D. (1979): A dynamic thermodynamic sea ice model. J. Phys. Oceanogr., **9**, 815–846.

HOLLOWAY, J. L., SPELMAN, M. J. and MANABE, S. (1973): Latitude-longitude grid suitable for numerical time integration of a global atmospheric model. Mon. Weather Rev., **101**, 69–78.

PARKINSON, C. L. and WASHINGTON, W. M. (1979): A large-scale numerical model of sea ice. J. Geophys. Res., **84**, 311–337.

ROTHROCK, D. A. (1975): The steady drift of an incompressible Arctic ice cover. J. Geophys. Res., **80**, 387–397.

SAKAI, S. and IMAWAKI, S. (1980): Enkeikai ni okeru Rossby-Haurwitz ha (The Rossby-Haurwitz wave in a circular ocean). Tsukumo Chigaku (Tsukumo Earth Science), **15**, 19–26.

SEMTNER, A. J. (1976): Numerical simulation of the Arctic Ocean circulation. J. Phys. Oceanogr., **6**, 409–425.

(*Received April 2, 1981; Revised manuscript received June 2, 1981*)